

Similar conclusions have been reached by Veillard and co-workers.<sup>33</sup> Thus, ignoring the token solvent ligand of the sixth coordination site, we would predict **6** to be thermodynamically more stable than **5**.

Both kinetic and thermodynamic factors therefore favor the *cis* intermediate **6**, as is widely observed for substitution by ligands which do not pose stringent steric demands. A qualitative diagram of potential energy and reaction coordinate is shown in Figure 6.

### Conclusions

We have shown how time-resolved IR spectroscopy has provided positive confirmation that both isomers of  $[LW(CO)_4(s)]$  (**5** and **6**) are the important intermediates in the photolysis of  $LW(CO)_5$  and *cis*-(pip) $LW(CO)_4$  compounds. **5** and **6** react with CO at different rates, indicating that these isomers are not stereochemically interconvertible on the time scale of their reaction with CO even in a solvent as nonpolar as *n*-heptane. The values of the rate constants suggest that the *n*-heptane is acting as a *Token Ligand* filling the vacant coordination site of the  $[LW(CO)_4(s)]$  species.

(33) Daniel, C.; Veillard, A. *Nouv. J. Chim.*, in press.

It is reasonable to suppose that the presence of the token ligand inhibits *trans*  $\rightleftharpoons$  *cis* isomerization of the  $[LW(CO)_4(s)]$  species examined here. It will therefore be of interest to investigate such isomerization in other metal carbonyl intermediates, particularly as a function of the solvent and of the transition metal. It will also be important to investigate in detail how the token ligand is exchanged and the precise nature of solvent-metal interactions in these intermediates.

**Acknowledgment.** We are grateful to SERC, the Paul Instrument Fund of the Royal Society, EEC, NATO (Grant No. 591/83), and Applied Photophysics Ltd. for supporting this research. The financial support of the National Science Foundation (Grant CHE 84-15153) and the Robert A. Welch Foundation (Grant No. B-434) is also greatly appreciated. G.R.D. thanks North Texas State University (NTSU) for a faculty development leave and the SERC for a Fellowship. We thank Professor J. K. Burdett, Dr. G. Davidson, A. J. Dixon, J. G. Gamble, Dr. F.-W. Grevels, R. E. Parsons, W. E. Porter, and J. M. Whalley for their help and advice.

(34) Creaven, B. S.; Dixon, A. J.; Kelly, J. M.; Long, C.; Poliakoff, M. *Organometallics*, submitted for publication.

## Chemisorption and Reaction of Ethylene on Chemically Modified Ru(001) Surfaces

M. M. Hills, J. E. Parmeter,<sup>†</sup> and W. H. Weinberg\*

Contribution from the Division of Chemistry and Chemical Engineering, California Institute of Technology, Pasadena, California 91125. Received December 9, 1986

**Abstract:** The adsorption and reaction of ethylene on a Ru(001) surface on which ordered  $p(2 \times 2)$  and  $p(1 \times 2)$  overlayers of oxygen adatoms are present have been investigated using high-resolution electron energy loss spectroscopy, thermal desorption mass spectrometry, and low-energy electron diffraction. In contrast to the di- $\sigma$ -bonded ethylene that is observed on clean Ru(001), ethylene chemisorbs molecularly in a  $\pi$ -bonded configuration at temperatures below 200 K on both the Ru(001)- $p(2 \times 2)O$  and Ru(001)- $p(1 \times 2)O$  surfaces. All of the ethylene that is chemisorbed on Ru(001)- $p(1 \times 2)O$  desorbs reversibly at 160 and 240 K, whereas approximately one-third of the ethylene on the Ru(001)- $p(2 \times 2)O$  surface desorbs molecularly at these temperatures. Upon annealing to 250 K, the irreversibly adsorbed ethylene on the Ru(001)- $p(2 \times 2)O$  surface dehydrogenates to ethylidyne ( $CCH_3$ ), which dehydrogenates further to vinylidene ( $CCH_2$ ) below 350 K. This represents the first unambiguous identification of a surface vinylidene species, as well as the first isolation of an intermediate in the decomposition of surface ethylidyne that preserves carbon-carbon bonding. The vinylidene decomposes to adsorbed carbon and methylidyne (CH) below 400 K, and the methylidyne decomposes with the evolution of hydrogen between 500 and 700 K.

### I. Introduction

Recent spectroscopic investigations of the interaction of ethylene and acetylene with the Ru(001) surface have revealed both the nature of the molecularly chemisorbed species and the decomposition products of these unsaturated hydrocarbons.<sup>1,2</sup> Co-adsorption experiments of hydrogen with ethylene, carbon monoxide with ethylene, and hydrogen with acetylene have clarified further the decomposition mechanisms.<sup>3,4</sup> The combined results of these studies<sup>5</sup> have led to the following mechanistic picture:<sup>1-5</sup> (1) both ethylene and acetylene chemisorb molecularly below 150 K on the Ru(001) surface, with rehybridization of the carbon atoms to nearly  $sp^3$  occurring; (2) upon heating to between 150 and 280 K, both ethylene and acetylene form a  $HCCH_2$  species, while acetylene also forms acetylide ( $CCH$ ) at these temperatures; (3) the  $HCCH_2$  species reacts rapidly to form acetylide and ethylidyne ( $CCH_3$ ); (4) the ethylidyne decomposes to carbon adatoms and hydrogen near 350 K, while the acetylide decomposes via car-

bon-carbon bond cleavage near 380 K, forming methylidyne (CH) and carbon adatoms; and (5) the methylidyne dehydrogenates, evolving hydrogen above approximately 500 K.

We report here the results of a study of the interaction of ethylene with Ru(001) surfaces on which preadsorbed overlayers of dissociatively adsorbed oxygen are present. We have concentrated on the reproducible and well-characterized Ru(001)- $p(2 \times 2)O$  and Ru(001)- $p(1 \times 2)O$  surfaces, although we have also examined the effects of disordered oxygen overlayers, the fractional coverages of which varied from approximately 0.05 to 0.5. The

(1) Hills, M. M.; Parmeter, J. E.; Mullins, C. B.; Weinberg, W. H. *J. Am. Chem. Soc.* 1986, 108, 3554.

(2) Parmeter, J. E.; Hills, M. M.; Weinberg, W. H. *J. Am. Chem. Soc.* 1986, 108, 3563.

(3) Hills, M. M.; Parmeter, J. E.; Weinberg, W. H. *J. Am. Chem. Soc.* 1986, 108, 7215.

(4) Parmeter, J. E.; Hills, M. M.; Weinberg, W. H. *J. Am. Chem. Soc.* 1987, 109, 72.

(5) Weinberg, W. H.; Parmeter, J. E.; Hills, M. M., in preparation.

<sup>†</sup> AT&T Bell Laboratories Predoctoral Fellow.

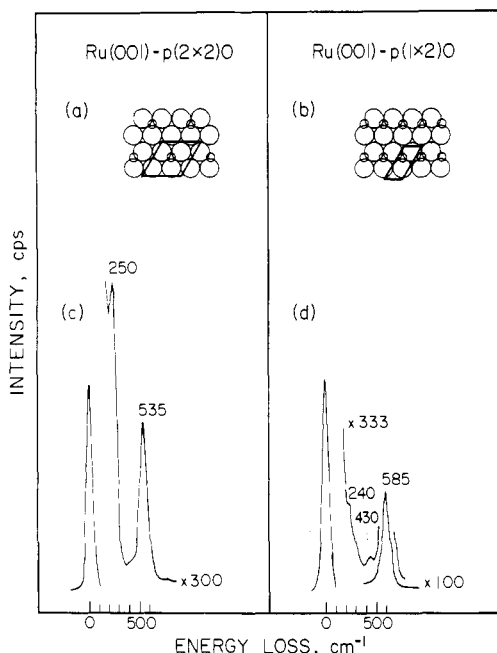


**Figure 1.** The structures and unit cells of the (a)  $p(2 \times 2)$  and (b)  $p(1 \times 2)$  ordered oxygen overlayers on the Ru(001) surface. Note that the oxygen occupies threefold hollow sites in both overlayers. Electron energy loss spectra of the (c)  $p(2 \times 2)$  and (d)  $p(1 \times 2)$  ordered oxygen overlayers.

$p(2 \times 2)$ O overlayer corresponds to a fractional surface coverage of oxygen adatoms of 0.25, while the  $p(1 \times 2)$ O overlayer consists of three independent domains that are rotated by  $120^\circ$  with respect to one another and corresponds to a fractional surface coverage of oxygen adatoms of 0.5.<sup>6,7</sup> These two structures are shown schematically in Figure 1, parts a and b. As may be seen in Figure 1, parts c and d, electron energy loss (EEL) spectra of the  $p(2 \times 2)$ O overlayer exhibit a  $\nu_s(\text{RuO})$  mode at  $535 \text{ cm}^{-1}$  and a surface phonon at  $250 \text{ cm}^{-1}$ .<sup>7</sup> Similarly, EEL spectra of the  $p(1 \times 2)$ O overlayer exhibit a  $\nu_s(\text{RuO})$  mode at  $585 \text{ cm}^{-1}$ , a surface phonon at  $240 \text{ cm}^{-1}$ , and a  $\nu_a(\text{RuO})$  mode at  $430 \text{ cm}^{-1}$ .<sup>7</sup> It is these spectroscopic signatures that render reproducible the synthesis of these two well-characterized surfaces.

There are several important reasons for our interest in this system. Oxygen overlayers increase the effective "Lewis acidity" of transition metal surfaces; i.e., the propensity of the surface metal atoms to accept electrons is increased. The extent of charge transfer from the ruthenium to the oxygen adatoms of the  $p(2 \times 2)$ O overlayer can be estimated using the observed change in the work function of  $+0.20 \text{ eV}$  following the adsorption of oxygen into the  $p(2 \times 2)$  overlayer<sup>6</sup> (making use of the previously determined ruthenium-oxygen bond length<sup>7</sup> and assuming that depolarization effects are negligible). It is found that approximately 0.03 electron is transferred from the ruthenium to each oxygen adatom of the overlayer. Similarly, it is estimated that approximately 0.04 electron is transferred from the ruthenium to each oxygen adatom of the  $p(1 \times 2)$  overlayer, using the measured change in the work function of  $+0.80 \text{ eV}$  and correcting for depolarization effects. This charge transfer increases the separation between the Fermi level of the ruthenium surface and the  $\pi^*$  orbital of ethylene, and this transfer could result in the adsorption of  $\pi$ -bonded ethylene on the oxygen precovered ruthenium surface by inhibiting back-donation into the  $\pi^*$  orbital. For example, the preadsorption of oxygen on Pd(100), Fe(111), Pt(111), and Ru(001)- $p(1 \times 2)$ O induces the formation of  $\pi$ -bonded molecular ethylene, as opposed to the di- $\sigma$ -bonded ethylene observed on the clean surfaces.<sup>8-11</sup> Furthermore, the charge

transfer from the ruthenium to the oxygen weakens both the metal-carbon and metal-hydrogen bonding and therefore could result in the formation of different intermediates in the ethylene decomposition reaction, possibly, although not necessarily, via the formation of oxygen-containing intermediates. Finally, the coadsorption of oxygen and ethylene permits a quantification of the extent of poisoning of molecular chemisorption of ethylene by both ordered and disordered oxygen overlayers, as well as the reduction in the extent of ethylene decomposition compared to the reduced (clean) surface.

## II. Experimental Procedures

Thermal desorption mass spectrometry and low-energy electron diffraction (LEED) measurements were carried out in an ultrahigh-vacuum (UHV) apparatus that has been described in detail previously.<sup>12</sup> Briefly, the chamber is pumped by both a 220-L/s noble ion pump and a titanium sublimation pump, which reduce the base pressure to below  $10^{-10}$  torr. The crystal is cooled to below 100 K with liquid nitrogen, and linear heating rates of the crystal of 5–20 K/s are achieved via resistive heating controlled by a power supply that is interfaced with an LSI-11 DEC laboratory computer. This UHV chamber contains a UTI-100C quadrupole mass spectrometer enclosed in a glass envelope for selective sampling of gases that desorb from only the well-oriented front surface of the single crystal.<sup>13</sup> Low-energy electron diffraction optics and a rotatable Faraday cup are available for the display of LEED patterns and the measurement of LEED beam profiles. A single-pass cylindrical mirror electron energy analyzer with an integral electron gun is available for Auger electron spectroscopy.

A second UHV chamber was used to conduct high-resolution electron energy loss spectroscopic (EELS) measurements. This chamber also has a base pressure below  $10^{-10}$  torr using similar pumping techniques, and liquid nitrogen cooling and resistive heating of the crystal were similarly employed. The home-built Kuyatt-Simpson-type EEL spectrometer has been described in detail elsewhere.<sup>14,15</sup> It was operated such that the kinetic energy of the electron beam incident upon the crystal was approximately 4 eV, at an angle of incidence of  $60^\circ$  with respect to the surface normal. The spectra were measured with a resolution of 60–80  $\text{cm}^{-1}$  (full-width at half-maximum of the elastically scattered peak), while maintaining a count rate of  $1-3 \times 10^5$  cps in the elastic channel. This UHV chamber also contains a quadrupole mass spectrometer, but it was not, in general, employed in the thermal desorption measurements reported here.

The techniques used for orienting, cutting, polishing, and mounting the Ru(001) crystals have been described previously.<sup>14,15</sup> The crystals were cleaned using periodic argon ion sputtering and routine annealing to 1000 K in  $7 \times 10^{-8}$  torr of  $\text{O}_2$ , followed by annealing to 1700 K in vacuo. Surface cleanliness was monitored in the two UHV chambers by Auger electron spectroscopy, EELS, and hydrogen thermal desorption.

Research purity (99.98% min) oxygen ( $^{16}\text{O}_2$ ) and CP grade (99.5%) ethylene were obtained from Matheson. The ethylene was purified further by three freeze-thaw-pump cycles. Research purity (99.98% min oxygen, 99%  $^{18}\text{O}_2$ ) isotopically labeled oxygen was obtained from Merck and Co. The purity of all gases was verified in situ by mass spectrometry in both chambers. Gas exposures are reported in units of Langmuirs, where 1 Langmuir =  $1 \text{ L} \equiv 10^{-6}$  torr-s. The quoted exposures have not been corrected for the relative ionization probabilities of the different gases.

## III. Results

**A. Molecularly Chemisorbed Ethylene on the Ru(001)- $p(2 \times 2)$ O and Ru(001)- $p(1 \times 2)$ O Surfaces.** The ordered  $p(2 \times 2)$  and  $p(1 \times 2)$  oxygen overlayers were synthesized on the Ru(001) surface by exposing the crystal at 90 K to 0.8 and 3 L of  $\text{O}_2$ , respectively, followed by annealing to 400 K. The existence of these ordered overlayers was verified both by LEED<sup>6</sup> and by EELS,<sup>7</sup> and their structures are shown in Figure 1, together with the corresponding EEL spectra.

Exposure of the Ru(001)- $p(2 \times 2)$ O and Ru(001)- $p(1 \times 2)$ O surfaces at 80 K to 2 L or more of ethylene gives rise to a mo-

(6) Madey, T. E.; Engelhardt, H. A.; Menzel, D. *Surf. Sci.* **1975**, *48*, 304.  
 (7) Rahman, T. S.; Anton, A. B.; Avery, N. R.; Weinberg, W. H. *Phys. Rev. Lett.* **1983**, *51*, 1979.  
 (8) Stuve, E. M.; Madix, R. J.; Brundle, C. R. *Surf. Sci.* **1985**, *152/153*, 532.  
 (9) Seip, U.; Tsai, M.-C.; Küppers, J.; Ertl, G. *Surf. Sci.* **1984**, *147*, 65.

(10) Steininger, H.; Ibach, H.; Lehwald, S. *Surf. Sci.* **1982**, *117*, 685.  
 (11) Barteau, M. A.; Broughton, J. Q.; Menzel, D. *Appl. Surf. Sci.* **1984**, *19*, 92.  
 (12) Williams, E. D.; Weinberg, W. H. *Surf. Sci.* **1979**, *82*, 93.  
 (13) Feulner, P.; Menzel, D. *J. Vac. Sci. Technol.* **1980**, *17*, 662.  
 (14) Thomas, G. E.; Weinberg, W. H. *J. Chem. Phys.* **1979**, *70*, 954.  
 (15) Thomas, G. E.; Weinberg, W. H. *Rev. Sci. Instrum.* **1979**, *50*, 497.

**Table I.** Comparison of Vibrational Frequencies (in  $\text{cm}^{-1}$ ) of  $\pi$ -Bonded Ethylene on the Ru(001)-p(2 $\times$ 2)O and Ru(001)-p(1 $\times$ 2)O Surfaces at 200 K with Other Ethylene Species

mode	Ru(001)-p(2 $\times$ 2)O and -p(1 $\times$ 2)O	multilayer C <sub>2</sub> H <sub>4</sub> on Ru(001) <sup>a</sup>	di- $\sigma$ -bonded C <sub>2</sub> H <sub>4</sub> on Ru(001) <sup>a</sup>	C <sub>2</sub> H <sub>4</sub> (g) <sup>b</sup>	Zeise's salt K[PtCl <sub>3</sub> (C <sub>2</sub> H <sub>4</sub> )] <sup>c</sup>	C <sub>2</sub> H <sub>4</sub> on Pd(100) + 0.18 ML of O <sup>d</sup>	C <sub>2</sub> H <sub>4</sub> on Fe(111) + 1 L of O <sub>2</sub> <sup>e</sup>	C <sub>2</sub> D <sub>4</sub> on Pt(111) + 0.23 ML of O <sup>f</sup>
C <sub>2</sub> H <sub>4</sub>								
$\nu_s$ (CM)	440		460		403			
$\nu_a$ (CM)					490			
$\rho$ (CH <sub>2</sub> )		860	775	810	841			
$\tau$ (CH <sub>2</sub> )			900					
$\omega$ (CH <sub>2</sub> )	950	970	1145	950	975	940	985	
$\delta$ (CH <sub>2</sub> )	1245 } 1520 } 3040 } 3040 } 3040 }	1350/1460	1450	1342/1444	1243 } 1515 } 3013 } 3075 }	1510	1290 } 1565 }	
$\nu$ (CC)		1630	1040	1623				
$\nu_s$ (CH <sub>2</sub> )		3000	2940	2989/3026		3020	3045	
$\nu_a$ (CH <sub>2</sub> )		3095	3050	3104				
C <sub>2</sub> D <sub>4</sub>								
$\nu_s$ (CM)								
$\nu_a$ (CM)								
$\rho$ (CD <sub>2</sub> )				1009/586	597/525			
$\tau$ (CD <sub>2</sub> )			700	728				
$\omega$ (CD <sub>2</sub> )	695	735	900	720/780	757			
$\delta$ (CD <sub>2</sub> )	975	1015/1125	1210	981/1078	962	985		970
$\nu$ (CC)	1350	1550	1040	1515	1353	1340		1370
$\nu_s$ (CD <sub>2</sub> )	2220	2310	2210	2251/2200	2224	2270		2230
$\nu_a$ (CD <sub>2</sub> )	2300		2295	2304/2345	2331			2340

<sup>a</sup>From ref 1. <sup>b</sup>From ref 7. <sup>c</sup>From refs 16 and 19. <sup>d</sup>From ref 8. <sup>e</sup>From ref 9. <sup>f</sup>From ref 10. <sup>g</sup>Coupled.

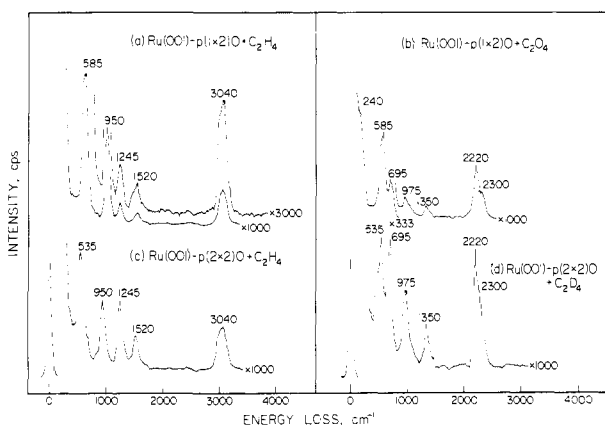


**Figure 2.** The EEL spectra that result from 2 L exposures of (a) C<sub>2</sub>H<sub>4</sub> and (b) C<sub>2</sub>D<sub>4</sub> on the Ru(001)-p(1 $\times$ 2)O surface, and (c) C<sub>2</sub>H<sub>4</sub> and (d) C<sub>2</sub>D<sub>4</sub> on the Ru(001)-p(2 $\times$ 2)O surface at 80 K, followed by heating to 200 K. These spectra are characteristic of  $\pi$ -bonded molecular ethylene on both surfaces.

lular multilayer that is identical with that observed on the clean surface.<sup>1</sup> This multilayer desorbs at 115 K, leaving a chemisorbed overlayer composed of the oxygen adatoms and  $\pi$ -bonded molecular ethylene. Submonolayer coverages of ethylene adsorbed at 80 K are also  $\pi$ -bonded. Low-energy electron diffraction patterns of these overlayers of molecularly chemisorbed ethylene continue to exhibit the indistinguishable p(2 $\times$ 2) and p(1 $\times$ 2) superstructures due to the oxygen adatoms. Figure 2a,b shows EEL spectra of C<sub>2</sub>H<sub>4</sub> and C<sub>2</sub>D<sub>4</sub> coadsorbed with the p(1 $\times$ 2)O overlayer at 80 K and annealed to 200 K, while Figure 2c,d shows EEL spectra of C<sub>2</sub>H<sub>4</sub> and C<sub>2</sub>D<sub>4</sub> coadsorbed with the p(2 $\times$ 2)O overlayer at 80 K and annealed to 200 K. These spectra indicate that  $\pi$ -bonded molecular ethylene is formed on both surfaces. The intense  $\nu_s$ (RuO) mode appears at 855  $\text{cm}^{-1}$  in Figure 2a,b and at 535  $\text{cm}^{-1}$  in Figure 2c,d. The  $\nu_a$ (RuO) mode is not resolved from the  $\nu_s$ (RuO) mode in Figure 2a,b, nor are the surface phonons resolved from the elastic peak in Figure 2a,c,d. The peaks in the spectra of Figure 2 that are due to  $\pi$ -bonded ethylene are assigned as follows. The intense feature at 950  $\text{cm}^{-1}$  (695  $\text{cm}^{-1}$  for C<sub>2</sub>D<sub>4</sub>) is the CH<sub>2</sub> (CD<sub>2</sub>) wagging mode. The peak at 3040  $\text{cm}^{-1}$  in Figure 2a,c is the symmetric carbon-hydrogen stretching mode from which the asymmetric stretching mode was not resolved. These modes were resolved in the EEL spectra of deuterated ethylene (cf. Figure 2b,d), with  $\nu_s$ (CD<sub>2</sub>) observed at 2220  $\text{cm}^{-1}$  and  $\nu_a$ (CD<sub>2</sub>) at 2300  $\text{cm}^{-1}$ . The frequencies of the carbon-hydrogen (car-

bon-deuterium) stretching modes as well as the CH<sub>2</sub> (CD<sub>2</sub>) wagging modes are indicative of nearly sp<sup>2</sup>-hybridized carbon atoms in the adsorbed ethylene. The modes at 1245 and 1520  $\text{cm}^{-1}$  in the EEL spectra of chemisorbed C<sub>2</sub>H<sub>4</sub> are the strongly coupled CH<sub>2</sub> scissoring and carbon-carbon stretching modes. The CD<sub>2</sub> scissoring and carbon-carbon stretching modes are essentially uncoupled in the spectra of deuterated ethylene and occur at 975 and 1350  $\text{cm}^{-1}$ , respectively. The frequency of the  $\nu$ (CC) mode in the spectra of deuterated ethylene indicates that this species is  $\pi$ -bonded to the surface. The strong coupling of the CH<sub>2</sub> scissoring and carbon-carbon stretching modes in the  $\pi$ -bonded C<sub>2</sub>H<sub>4</sub> is in agreement with the observed coupling of these modes of C<sub>2</sub>H<sub>4</sub> in Zeise's salt.<sup>16,18,19</sup> Although not resolved from the ruthenium-oxygen stretching mode in Figure 2a-d, the  $\nu$ (Ru-C<sub>2</sub>H<sub>4</sub>) mode was observed at 440  $\text{cm}^{-1}$  in EEL spectra measured 10° off-specular, in which the  $\nu_s$ (RuO) mode exhibits a much lower intensity due to its largely dipolar character and strong dynamic dipole and in which the elastic peak has also decreased in intensity.

These mode assignments are compared in Table I with those of multilayer and di- $\sigma$ -bonded ethylene on Ru(001), C<sub>2</sub>H<sub>4</sub>(g), Zeise's salt, and  $\pi$ -bonded, molecularly chemisorbed ethylene on other group 8 transition metal surfaces.<sup>1,8-10,16,17,19</sup> These comparisons confirm that molecularly chemisorbed ethylene on both Ru(001)-p(2 $\times$ 2)O and Ru(001)-p(1 $\times$ 2)O is  $\pi$ -bonded to the surfaces and that the carbon atoms of the ethylene are very nearly sp<sup>2</sup>-hybridized, as judged by the frequencies of the  $\nu_s$ (CH<sub>2</sub>),  $\nu_s$ (CD<sub>2</sub>),  $\nu_a$ (CD<sub>2</sub>), and  $\nu$ (CC) (of C<sub>2</sub>D<sub>4</sub>) modes, as well as the good agreement of all mode assignments with those of Zeise's salt, a paradigm of  $\pi$ -bonded ethylene. On the other hand, the carbon atoms of di- $\sigma$ -bonded ethylene on the Ru(001) surface are almost completely rehybridized to sp<sup>3</sup>, as judged by the significantly lower frequencies of the carbon-carbon and carbon-hydrogen stretching modes, and the upshifts in the CH<sub>2</sub> and CD<sub>2</sub> wagging modes.

Annealing the  $\pi$ -bonded ethylene on the Ru(001)-p(1 $\times$ 2)O surface above 240 K results in the reversible molecular desorption of all of the ethylene. This was demonstrated both by EEL spectra that were measured following the annealing of adsorbed ethylene overlayers to 240 K, which exhibited only the  $\nu_s$ (RuO),  $\nu_a$ (RuO), and phonon modes as in Figure 1d, and by thermal desorption spectra of these overlayers that showed only the desorption of

(16) Powell, D. B.; Scott, J. G. V.; Sheppard, N. *Spectrochim. Acta, Part A* **1972**, *28*, 327.

(17) Shimanouchi, T. *NSRDS-NBS Publ.* **1972**, *39*, 74.

(18) Powell et al. believe that there is considerable  $\nu$ (CC) and  $\delta$ (CH<sub>2</sub>) character in both the 1243- and 1515- $\text{cm}^{-1}$  bands of Zeise's salt.<sup>15</sup>

(19) Hiraishi, J., *Spectrochim. Acta, Part A* **1969**, *25*, 749.

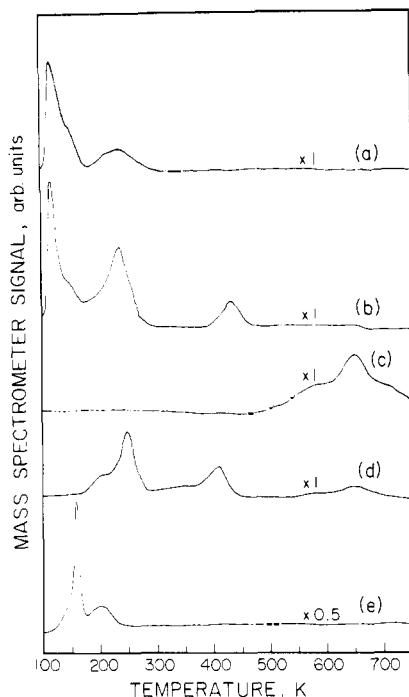


**Figure 3.** (a) The ethylene (mass 28) thermal desorption spectrum following a 6 L exposure of C<sub>2</sub>H<sub>4</sub> on the Ru(001)-p(1×2)O surface at 90 K. (b) The ethylene and C<sup>16</sup>O (mass 28), (c) the C<sup>18</sup>O (mass 30), and (d) the hydrogen (mass 2) thermal desorption spectra following a 4 L exposure of C<sub>2</sub>H<sub>4</sub> on the Ru(001)-p(2×2)<sup>18</sup>O surface at 90 K. (e) The hydrogen (mass 2) thermal desorption spectrum following a 10 L exposure of H<sub>2</sub> on the Ru(001)-p(2×2)O surface at 90 K.

molecularly chemisorbed ethylene in a shoulder and a peak centered at 160 and 240 K, respectively, and the desorption of the molecular ethylene multilayer at 115 K (cf. Figure 3a). The fractional saturation coverage of ethylene chemisorbed on Ru(001)-p(1×2)O was estimated to be 0.10 from the ethylene thermal desorption spectra. The activation energy of desorption (equal to the heat of adsorption since the adsorption is unactivated) of ethylene desorbing in the 160 K peak is approximately  $9.8 \pm 1$  kcal/mol, and that of ethylene desorbing in the 240 K peak is approximately  $14.0 \pm 1$  kcal/mol, assuming preexponential factors of the desorption rate coefficients of  $10^{13}$ – $10^{14}$  s<sup>-1</sup>.<sup>20</sup>

In contrast to the completely reversible adsorption of ethylene on the Ru(001)-p(1×2)O surface, only one-third of the chemisorbed ethylene on the Ru(001)-p(2×2)O surface desorbs reversibly from a saturated overlayer, the total fractional coverage of which is 0.12. As shown in Figure 3b, this reversibly adsorbed ethylene also desorbs in a peak at 240 K and a shoulder at 160 K on the multilayer peak. This thermal desorption measurement was conducted using a p(2×2)<sup>18</sup>O overlayer in order to distinguish molecularly desorbed ethylene from C<sup>18</sup>O that is produced by the surface reaction between carbon (from the decomposition of ethylene) and oxygen (cf. Figure 3c). However, a small concentration of C<sup>16</sup>O due to background adsorption (fractional surface coverage between 0.01 and 0.02) is also observed to desorb, as indicated by the desorption-limited peak at approximately 450 K in Figure 3b.

Although molecularly chemisorbed ethylene on both the Ru(001)-p(2×2)O and Ru(001)-p(1×2)O surfaces desorbs in two peaks at 160 and 240 K, EEL spectra that were measured after annealing to temperatures between 115 and 240 K were identical and indicative of  $\pi$ -bonded ethylene. The identification of the ethylene that desorbs in the 160 K peak as a  $\pi$ -bonded species implies that this peak does not correspond to desorption of a second layer of ethylene.

#### B. Thermal Decomposition of Ethylene on the Ru(001)-p(2×2)O Surface and on Disordered Oxygen Overlayers on the

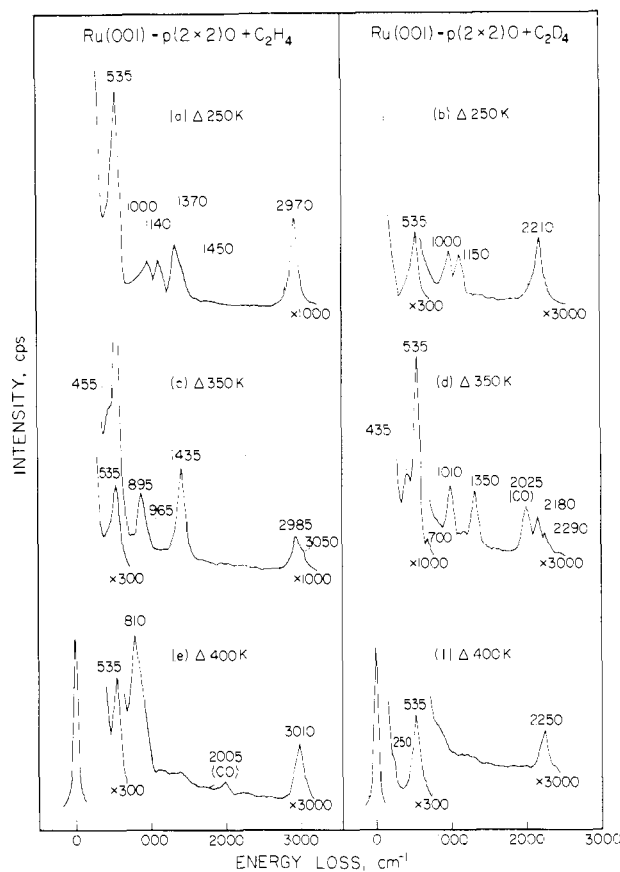


**Figure 4.** The EEL spectra that result from 2 L exposures of C<sub>2</sub>H<sub>4</sub> (a, c, e) and C<sub>2</sub>D<sub>4</sub> (b, d, f) on the Ru(001)-p(2×2)O surface at 80 K and heated to (a, b) 250 K, (c, d) 350 K, and (e, f) 400 K.

**Ru(001) Surface.** Electron energy loss spectra which demonstrate the effect of annealing the molecularly chemisorbed ethylene overlayer on the Ru(001)-p(2×2)O surface to higher temperatures are shown in Figure 4. Comparing the spectra of  $\pi$ -bonded ethylene annealed to 200 K (Figure 2c,d) to those of the same overlayers annealed to 250 K (Figure 4a,b) indicates that by 250 K the ethylene has converted completely to a new species which can be identified easily as ethylidyne. In fact,  $\pi$ -bonded ethylene reacts to yield ethylidyne at temperatures as low as 230 K. Ethylidyne is formed also from the decomposition of di- $\sigma$ -bonded ethylene on the Ru(001) surface<sup>1</sup> and is characterized by carbon-carbon stretching and symmetric methyl deformation modes at 1140 and 1370 cm<sup>-1</sup> for CCH<sub>3</sub>, and at 1150 and 1000 cm<sup>-1</sup> for CCD<sub>3</sub>. The symmetric and asymmetric carbon-hydrogen stretching modes, expected at 2945 and 3045 cm<sup>-1</sup> (2190 and 2280 cm<sup>-1</sup> for CCD<sub>3</sub>), were not resolved in these spectra, but appear as a single feature at 2970 cm<sup>-1</sup> (2210 cm<sup>-1</sup> for CCD<sub>3</sub>). The asymmetric methyl deformation mode and the methyl rocking mode appear at 1450 and 1000 cm<sup>-1</sup>, respectively, in Figure 4a, but are not resolved from the  $\delta_s$ (CD<sub>3</sub>) and  $\nu_3$ (RuO) modes at 1000 and 535 cm<sup>-1</sup> in Figure 4b. The  $\nu$ (Ru≡CCH<sub>3</sub>) mode of adsorbed ethylidyne, expected at 480 cm<sup>-1</sup>, is not resolved from the  $\nu_3$ (RuO) mode in either of the spectra of Figure 4a,b. These mode assignments of adsorbed ethylidyne have been discussed in detail elsewhere.<sup>1</sup>

Electron energy loss spectra that were measured following annealing this overlayer to 350 K (Figure 4c,d) demonstrate the total conversion of the ethylidyne to a new species, as judged both by the disappearance of the carbon-carbon stretching modes of CCH<sub>3</sub> and CCD<sub>3</sub> at 1140 and 1150 cm<sup>-1</sup> and the CH<sub>3</sub> rocking mode at 1000 cm<sup>-1</sup>, as well as by the appearance of new modes which are attributed to a nearly sp<sup>2</sup>-hybridized vinylidene (CCH<sub>2</sub>). The EEL spectrum of the deuterated vinylidene (Figure 4d) exhibits three intense peaks at 700, 1010, and 1350 cm<sup>-1</sup>. The peak at 1350 cm<sup>-1</sup> may be assigned unambiguously to the stretching mode of a carbon-carbon double bond since it is far

**Table II.** Comparison of Vibrational Frequencies (in  $\text{cm}^{-1}$ ) of  $\text{CCH}_2$  on the  $\text{Ru}(001)\text{-p}(2\times 2)\text{O}$  Surface with Other  $\text{CCH}_2$  Species

mode	$\text{CCH}_2$ on $\text{Ru}(001)\text{-p}(2\times 2)\text{O}$	$\text{CCD}_2$ on $\text{Ru}(001)\text{-p}(2\times 2)\text{O}$	$\text{CCH}_2$ in $\text{Os}_3\text{H}_2(\text{CO})_9(\text{CCH}_2)^c$	$\text{CCH}_2$ on $\text{Pd}(111)^d$	$\text{Pt}(111)^e$
$\nu(\text{Ru-C})$	455	435	255–311	n.r.	n.r.
$\tau(\text{CH}_2)$ or $(\text{CD}_2)$	n.r. <sup>a</sup>	n.r.	808	n.r.	n.r.
$\omega(\text{CH}_2)$ or $(\text{CD}_2)$	895	700	959	n.r.	900
$\rho(\text{CH}_2)$ or $(\text{CD}_2)$	965	n.r.	1048	n.r.	n.r.
$\delta(\text{CH}_2)$ or $(\text{CD}_2)$	1435	1010	1467 } <sup>b</sup>	n.r.	1420
$\nu(\text{CC})$	1435	1350	1328 } <sup>b</sup>	1328	1100
$\nu_s(\text{CH}_2)$ or $(\text{CD}_2)$	2985	2180	2990	2986	2970
$\nu_a(\text{CH}_2)$ or $(\text{CD}_2)$	3050	2290	3052	n.r.	n.r.

<sup>a</sup>n.r. = not resolved. <sup>b</sup>Coupled. <sup>c</sup>From ref 22. <sup>d</sup>From ref 23. <sup>e</sup>From ref 24.

too high in frequency to correspond either to any carbon–deuterium deformation mode or to  $\nu(\text{CC})$  of a single bond. The loss features at 700 and 1010  $\text{cm}^{-1}$  are assigned to the  $\text{CD}_2$  wagging and scissoring modes. The other loss peaks at 435, 2180, and 2290  $\text{cm}^{-1}$  are then assigned easily as the  $\nu(\text{Ru}=\text{CCD}_2)$ ,  $\nu_s(\text{CD}_2)$ , and  $\nu_a(\text{CD}_2)$  modes of the  $\text{CCD}_2$ . The  $\nu(\text{CO})$  mode of a small concentration of carbon monoxide that is due to adsorption from the background of the UHV chamber appears at 2035  $\text{cm}^{-1}$  in Figure 4d. This CO corresponds to a fractional surface coverage of less than 0.02,<sup>21</sup> contributes slightly to the loss peak at 435  $\text{cm}^{-1}$ , and has no effect upon the other adsorbates.

The EEL spectrum of the corresponding hydrogenic species ( $\text{CCH}_2$ ) in Figure 4c exhibits two clearly resolved peaks at 895 and 1435  $\text{cm}^{-1}$ . The peak at 895  $\text{cm}^{-1}$  is due to the  $\text{CH}_2$  wagging mode that has shifted up from 700  $\text{cm}^{-1}$  in the deuterated spectrum. The more intense loss feature at 1435  $\text{cm}^{-1}$  results from two overlapping peaks that correspond to the carbon–carbon stretching mode and the  $\text{CH}_2$  scissoring mode that have shifted up from 1350 and 1010  $\text{cm}^{-1}$ , respectively, in  $\text{CCD}_2$ . The other loss peaks at 455, 2985, and 3050  $\text{cm}^{-1}$  are the  $\nu(\text{Ru}=\text{CCH}_2)$ ,  $\nu_s(\text{CH}_2)$ , and  $\nu_a(\text{CH}_2)$  modes of  $\text{CCH}_2$ . The  $\text{CH}_2$  rocking mode is also evident at 965  $\text{cm}^{-1}$  in Figure 4c, although the  $\text{CD}_2$  rocking mode is not resolved from the  $\text{CD}_2$  wagging mode in the spectrum of  $\text{CCD}_2$  in Figure 4d.

The vibrational frequencies of this vinylidene are compared in Table II with those of vinylidene in an  $\text{Os}_3\text{H}_2(\text{CO})_9(\text{CCH}_2)$  cluster compound and to two other surface species that have been identified as  $\text{CCH}_2$ .<sup>22–24</sup> There is a good correspondence between the vibrational frequencies of the  $\text{CCH}_2$  in the cluster and the vinylidene that is present on the  $\text{Ru}(001)\text{-p}(2\times 2)\text{O}$  surface. The  $\text{CCH}_2$  ligand of the complex is bridge-bonded to two osmium atoms with  $\pi$ -electron donation from the carbon–carbon double bond to the third osmium atom, as shown schematically in Figure 5a.<sup>22</sup> The structure of this compound, determined by X-ray crystallography, is shown in Figure 5b.<sup>25</sup>

The existence of a  $\text{CCH}_2$  species on the  $\text{Ru}(001)\text{-p}(2\times 2)\text{O}$  surface following ethylene adsorption at 80 K and annealing to 350 K is confirmed further by the hydrogen thermal desorption spectrum, shown in Figure 3d, from ethylene adsorbed on the  $\text{Ru}(001)\text{-p}(2\times 2)^{18}\text{O}$  surface. Approximately half of the hydrogen desorbs below 350 K, indicating that the surface species present at 350 K has a stoichiometry of  $\text{C}_2\text{H}_2$ . The hydrogen that desorbs in the two peaks at 210 and 250 K therefore corresponds to hydrogen that results from the dehydrogenation of  $\pi$ -bonded ethylene to ethylidyne and the subsequent dehydrogenation of ethylidyne to vinylidene. As may be seen by comparing the hydrogen thermal desorption spectrum of Figure 3d with that of hydrogen adsorbed on the  $\text{Ru}(001)\text{-p}(2\times 2)\text{O}$  surface (Figure 3e), most of the hydrogen that results from the dehydrogenation of ethylene and ethylidyne desorbs above the temperature at which chemisorbed hydrogen desorbs from the  $\text{Ru}(001)\text{-p}(2\times 2)\text{O}$

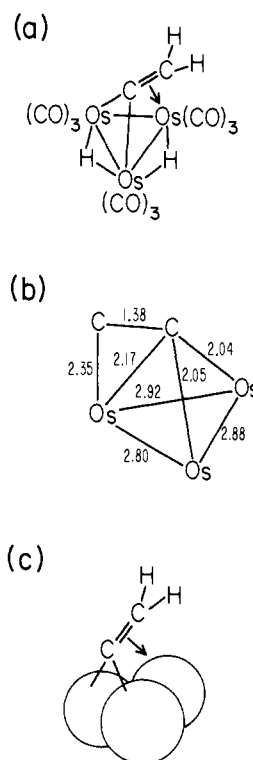


**Figure 5.** (a) The bonding configuration and (b) the structure of  $\text{CCH}_2$  in  $\text{Os}_3\text{H}_2(\text{CO})_9(\text{CCH}_2)$ .<sup>25</sup> (c) The analogous bonding configuration of  $\text{CCH}_2$  on the  $\text{Ru}(001)\text{-p}(2\times 2)\text{O}$  surface.

surface, and is therefore a reaction-limited desorption product.

The vinylidene could be rehydrogenated to ethylidyne, indicating that this reaction is reversible. After a saturation coverage of  $\text{CCH}_2$  was formed, the  $\text{Ru}(001)\text{-p}(2\times 2)\text{O}$  surface was cooled to 80 K, exposed to 10 L of hydrogen, and annealed to 200 K. Subsequently measured EEL spectra showed the presence of ethylidyne and a small amount of unreacted vinylidene, indicating that most of the  $\text{CCH}_2$  had been rehydrogenated. Annealing this overlayer to 350 K results in the dehydrogenation of the ethylidyne to vinylidene. In another experiment, the vinylidene was exposed to 15 L of deuterium at a surface temperature of 200–250 K. The EEL spectrum of this overlayer indicates the existence of different isotopes of ethylidyne. As expected, the species with the highest coverage is  $\text{CCH}_2\text{D}$  with a  $\delta_s(\text{CH}_2\text{D})$  mode at 1260  $\text{cm}^{-1}$ , whereas  $\text{CCH}_3$  is present at a lower coverage. Neither  $\text{CCD}_2\text{H}$  nor  $\text{CCD}_3$  was detected.

As shown in Figure 3d, annealing the vinylidene overlayer on the  $\text{Ru}(001)\text{-p}(2\times 2)\text{O}$  surface to higher temperatures causes further hydrogen desorption in a peak at 400 K, indicating that the  $\text{CCH}_2$  has dehydrogenated. Electron energy loss spectra of the overlayer that is formed by annealing the surface to 400 K (cf. Figure 4e,f) are consistent with this interpretation. The stable species on the surface at this temperature are carbon adatoms and methylidyne, which are formed via cleavage of the carbon–carbon bond and one carbon–hydrogen bond of vinylidene. No intermediates in the vinylidene decomposition reaction such as methylene ( $\text{CH}_2$ ) or acetylidyne ( $\text{CCH}$ ) were observed by EELS.

(21) This estimate is based on the intensity of the  $\nu(\text{CO})$  mode in this spectrum compared to those of low CO coverages on the  $\text{Ru}(001)$  surface.

(22) Andrews, J. R.; Kettle, S. F. A.; Powell, D. B.; Sheppard, N. *Inorg. Chem.* **1982**, *21*, 2874.

(23) Gates, J. A.; Kesmodel, L. L. *Surf. Sci.* **1983**, *124*, 68.

(24) Ibach, H.; Lehwald, S. *J. Vac. Sci. Technol.* **1978**, *15*, 407.

(25) Deeming, A. J.; Underhill, M. *J. Chem. Soc., Dalton Trans.* **1974**, 1415.

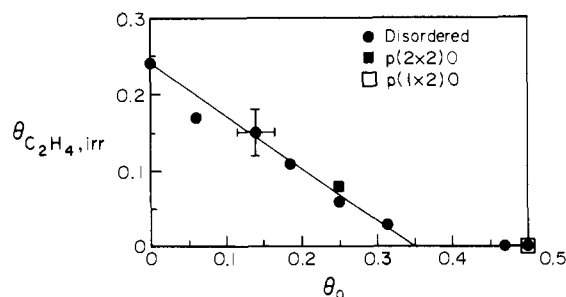


Figure 6. The inhibition of irreversible ethylene adsorption by preadsorbed oxygen adatoms.

The existence of methylidyne is indicated both by the presence of a carbon–hydrogen bending mode at  $810\text{ cm}^{-1}$  and a carbon–hydrogen stretching mode at  $3010\text{ cm}^{-1}$  in Figure 4e. The carbon–deuterium bending mode, expected at  $615\text{ cm}^{-1}$  for CD, overlaps and is unresolved from the intense  $\nu_s(\text{RuO})$  mode in Figure 4f. The carbon–deuterium stretching mode, observed at  $2250\text{ cm}^{-1}$ , is however, at the same frequency as that of methylidyne on the clean Ru(001) surface.<sup>1,2</sup> The  $\nu_s(\text{Ru}\equiv\text{CH})$  and  $\nu_s(\text{Ru}\equiv\text{CD})$  modes expected at  $465$  and  $415\text{ cm}^{-1}$  were not resolved from the  $\nu_s(\text{RuO})$  mode in these spectra. Note, however, that the phonon mode of the p(2x2) oxygen overlayer was resolved in the spectrum of Figure 4f.

Both the hydrogen thermal desorption spectra and the EEL spectra measured following annealing this overlayer to higher temperatures show that the methylidyne dehydrogenates between  $500$  and  $700\text{ K}$ . The surface carbon reacts with the oxygen adatoms ( $^{18}\text{O}$ ) to form  $\text{C}^{18}\text{O}$ , which desorbs above  $500\text{ K}$ , as shown in Figure 3c. This carbon monoxide desorption peak is reaction-limited, because this coverage of desorption-limited CO would appear at a much lower temperature (approximately  $430\text{ K}$ ) on this surface. Neither  $\text{CO}_2$  nor  $\text{H}_2\text{O}$  was observed to desorb from this overlayer, indicating that the adsorbed oxygen either reacted with carbon above  $500\text{ K}$  evolving CO or remained on the surface and desorbed only after annealing to  $1700\text{ K}$ . Because of the absence of both spectroscopically observed intermediates and mass spectrometrically detected reaction products, neither the ethylene, ethylidyne, vinylidene, nor methylidyne reacts with the oxygen adatoms on the Ru(001)–p(2x2)O surface.

Finally, the adsorption and reaction of saturation coverages of ethylene on disordered oxygen overlayers on Ru(001) have also been investigated. The disordered oxygen overlayers were prepared by exposing the Ru(001) surface to oxygen at  $80$ – $100\text{ K}$ . The fractional surface coverages of oxygen were estimated by using the linear relationship between coverage and exposure, and the known coverage of  $0.25$  corresponding to a  $0.8\text{ L}$  exposure of oxygen.<sup>26</sup> Hydrogen and ethylene thermal desorption spectra were used to evaluate the inhibition of reversible and irreversible ethylene adsorption by the preadsorbed oxygen. It was found that the fraction of ethylene that chemisorbs reversibly increases with increasing oxygen precoverage, while the amount of irreversibly adsorbed ethylene decreases approximately linearly with the oxygen precoverage. As shown in Figure 6, a fractional coverage of oxygen of approximately  $0.35$  inhibits ethylene decomposition completely.

#### IV. Discussion

**A. Molecularly Chemisorbed Ethylene.** It has been shown that ethylene chemisorbed on the Ru(001)–p(2x2)O and Ru(001)–p(1x2)O surfaces below  $230\text{ K}$  is a  $\pi$ -bonded molecular species, for example, by comparison of the vibrational spectra to that of Zeise's salt. Calculations of the electronic structure of Zeise's anion have suggested that donation of electron density from the  $\pi$  orbital of ethylene to the platinum accounts for at least  $75\%$  of the total bonding of the ethylene ligand to the platinum, while back-donation from the platinum d orbitals to the ethylene  $\pi^*$

orbital accounts for the rest.<sup>27</sup> The occurrence of a small amount of back-bonding in Zeise's salt is consistent with neutron diffraction results, which show that the hydrogen atoms are bent away from the metal atom such that the carbon atoms are positioned  $0.16\text{ \AA}$  away from the plane of the four hydrogen atoms and toward the platinum atom.<sup>28</sup> If no back-bonding were to occur, the hydrogen and carbon atoms would remain coplanar. By analogy to Zeise's salt, the bonding of ethylene to these modified ruthenium surfaces may be described in terms of the donation of electron density from the  $\pi$  orbital of ethylene to the d band of the ruthenium of which the local density of unoccupied states has been increased by the presence of the electronegative oxygen adatoms, and the simultaneous back-donation of a small amount of electron density from the ruthenium surface to the  $\pi^*$  orbital of chemisorbed ethylene.

The ability of ethylene to act both as a  $\pi$  donor and a  $\pi^*$  acceptor lowers the vibrational frequency of the carbon–carbon stretching mode of chemisorbed,  $\pi$ -bonded  $\text{C}_2\text{D}_4$  to  $1350\text{ cm}^{-1}$  and of  $\text{C}_2\text{D}_4$  in Zeise's salt to  $1353\text{ cm}^{-1}$  from the gas-phase value of  $1515\text{ cm}^{-1}$ . The frequency of the carbon–carbon stretching mode of  $\pi$ -bonded  $\text{C}_2\text{H}_4$  cannot be compared to that of  $\text{C}_2\text{H}_4(\text{g})$  owing to the previously discussed coupling of the  $\delta(\text{CH}_2)$  and  $\nu(\text{CC})$  modes of the chemisorbed ethylene. However, the frequencies of these two modes agree with those of the ethylene ligand in Zeise's salt, suggesting that the degree of mode coupling and the bonding are similar in the two species. The bonding of ethylene to platinum in Zeise's salt increases the carbon–carbon bond length to  $1.375\text{ \AA}$  from  $1.337\text{ \AA}$  in gaseous ethylene,<sup>28</sup> and a similar lengthening of this bond is expected to occur in the ethylene that is  $\pi$ -bonded to the Ru(001)–p(1x2)O and Ru(001)–p(2x2)O surfaces.

Previous investigations<sup>1,3</sup> of ethylene adsorbed on clean, hydrogen precovered, and CO-precovered Ru(001) surfaces have shown that the molecularly chemisorbed ethylene is di- $\sigma$ -bonded with a carbon–carbon stretching frequency of  $1040\text{ cm}^{-1}$ . Hence, the carbon atoms of di- $\sigma$ -bonded ethylene on the Ru(001) surface are essentially  $\text{sp}^3$ -hybridized, whereas those of  $\pi$ -bonded ethylene on the Ru(001)–p(2x2)O and Ru(001)–p(1x2)O surfaces are more nearly  $\text{sp}^2$ -hybridized. The change in the hybridization of the carbon atoms of adsorbed ethylene from  $\text{sp}^3$  as observed on the clean surface to nearly  $\text{sp}^2$  as observed on the oxygen precovered surfaces has also been observed for coadsorbed ethylene and oxygen on the Pd(100), Fe(111), and Pt(111) surfaces.<sup>8–10,29</sup> Moreover, the observed vibrational frequencies of these  $\pi$ -bonded ethylene species agree quite well with those of  $\pi$ -bonded ethylene on the Ru(001)–p(2x2)O and Ru(001)–p(1x2)O surfaces, as shown in Table I. Our results are also in agreement with those of Barteau et al.<sup>11</sup> for ethylene chemisorbed on the Ru(001)–p(1x2)O surface at  $170\text{ K}$ .

Since there is no indication of any direct chemical interaction between the  $\text{C}_2\text{H}_4$  and the oxygen adatoms, the interaction between ethylene and the Ru(001), the Ru(001)–p(2x2)O and the Ru(001)–p(1x2)O surfaces may be discussed in terms of the "Lewis acidity" of the surface. When oxygen is adsorbed, the Lewis acidity of the surface, i.e., the ability of the ruthenium atoms to accept electrons, increases. As discussed in section I, approximately  $0.03$  electron is transferred from the ruthenium to each oxygen adatom of the p(2x2) overlayer, and  $0.04$  electron is transferred to each oxygen atom of the p(1x2) overlayer. This charge transfer increases the Lewis acidity of the surface ruthenium atoms, making  $\pi$ -donation from ethylene to the ruthenium more favorable and  $\pi^*$ -back-donation from the surface less favorable, and this alters the bonding of ethylene from di- $\sigma$ - to  $\pi$ -bonding. A similar effect has been observed when acetone is adsorbed below  $200\text{ K}$  on the Ru(001) and the Ru(001)–p(2x2)O surfaces.<sup>30</sup> On Ru(001), acetone forms largely a side-on bonded

(27) Rosch, N.; Messmer, R. P.; Johnson, K. H. *J. Am. Chem. Soc.* **1974**, *96*, 3855.

(28) Love, R. A.; Koetzle, T. F.; Williams, G. J. B.; Andrews, L. C.; Bau, R. *Inorg. Chem.* **1975**, *14*, 2653.

(29) In addition, a small amount of  $\pi$ -bonded ethylene is present on the clean Pd(100) surface.

(26) The linear dependence of coverage upon exposure has been shown by Mader et al.<sup>6</sup> to be appropriate for fractional oxygen coverages below  $0.35$ .

$\eta^2(\text{C},\text{O})-(\text{CH}_3)_2\text{CO}$  species, as well as a small amount of  $\eta^1$ -acetone, which is bonded through a lone pair of electrons on the oxygen atom. Addition of the  $p(2\times 2)\text{O}$  overlayer to the surface stabilizes the  $\eta^1$ -acetone with respect to the  $\eta^2$ -acetone, since the  $\eta^1$ -bonding configuration maximizes the net electron transfer from the acetone to the ruthenium. In both cases the increased Lewis acidity of the ruthenium surface increases the selectivity toward the adspecies which donate the most electron density and withdraw the least,  $\eta^1$ -acetone and  $\pi$ -bonded ethylene. Similar effects have been observed also for the coadsorption of oxygen with formaldehyde<sup>31</sup> and with formamide<sup>32</sup> on Ru(001).

On the other hand, the preadsorption of oxygen on Ru(001) does not alter the bonding of acetylene: the carbon atoms of acetylene are rehybridized to nearly  $sp^3$  on the Ru(001), Ru(001)- $p(2\times 2)\text{O}$ , and Ru(001)- $p(1\times 2)\text{O}$  surfaces.<sup>2,33</sup> This is a consequence of the different energy levels of the unoccupied  $\pi$  orbitals of gaseous ethylene ( $1b_{2g}$ ) and acetylene ( $\pi_g$ ), which lie at -2.85 and -6.1 eV with respect to the vacuum level, respectively.<sup>34,35</sup> Upon adsorption, these orbital energies will downshift and broaden. Analogously, ultraviolet photoelectron spectroscopic data of Demuth and Eastman<sup>36</sup> show that the bonding  $\pi$  orbitals,  $\pi_u$  of acetylene and  $b_{3u}$  of ethylene, shift from -11.4 to -13.1 eV and from -10.5 eV to -11.6 eV upon adsorption of  $\text{C}_2\text{H}_2$  and  $\text{C}_2\text{H}_4$  on Ni(111). The Fermi level of Ru(001) lies at -5.5 eV,<sup>37</sup> and the Fermi levels of Ru(001)- $p(2\times 2)\text{O}$  and Ru(001)- $p(1\times 2)\text{O}$  lie at -5.7 and -6.3 eV with respect to the vacuum (zero) level.<sup>6</sup> The energy of the  $\pi_g$  orbital of acetylene shifts below the Fermi level of all three surfaces upon adsorption such that back-donation to the empty  $\pi_g$  orbital of acetylene occurs, resulting in rehybridization of the carbon atoms to  $sp^3$ . Similarly, the energy of the  $\pi^*$  ( $1b_{2g}$ ) orbital of ethylene shifts sufficiently near the Fermi level of Ru(001) and broadens upon adsorption to facilitate back-donation, resulting in the formation of di- $\sigma$ -bonded ethylene on the clean surface. However, the Fermi levels of the two oxygen precovered surfaces are apparently too low in energy with respect to that of the  $\pi^*$  orbital to allow significant back-donation. Hence, ethylene adsorbed on these two surfaces is  $\pi$ -bonded.

The effect of oxygen adatoms upon the postadsorption of ethylene may be compared with that of carbon, which, like oxygen, is adsorbed in threefold hollow sites on Ru(001).<sup>7,38,39</sup> A fractional coverage of 0.25 carbon adatom (which is equal to the coverage of oxygen adatoms in the  $p(2\times 2)\text{O}$  overlayer) produced by the thermal decomposition of ethylene on Ru(001) results in less charge transfer compared to the  $p(2\times 2)$  oxygen overlayer owing to the similar electronegativities of ruthenium (2.2) and carbon (2.55), and the greater electronegativity of oxygen (3.44). Electron energy loss spectra of ethylene adsorbed on the Ru(001) surface precovered with a fractional coverage of 0.25 carbon adatom show that this ethylene is di- $\sigma$ -bonded,<sup>40</sup> confirming that the  $\pi$ -bonding of molecular ethylene induced by the  $p(2\times 2)$  oxygen overlayer results from an electronic perturbation of the surface.

In addition to the change in the nature of the bonding of chemisorbed ethylene on the Ru(001) surfaces modified chemically by oxygen adatoms, the total coverage of molecularly chemisorbed ethylene is also reduced. As shown by the ethylene and hydrogen thermal desorption spectra, a fractional coverage of oxygen adatoms of 0.5 reduces the saturation fractional coverage of chemisorbed ethylene to 0.10, all of which adsorbs reversibly (cf. a saturation fractional coverage of 0.30 on Ru(001) of which 0.06

desorbs reversibly). The observation that a larger fraction of  $\pi$ -bonded ethylene desorbs molecularly compared with di- $\sigma$ -bonded ethylene is in agreement with results for ethylene adsorbed on the clean and oxygen-precovered Pd(100), Fe(111), and Pt(111) surfaces.<sup>8-10</sup> Indeed, all of the  $\pi$ -bonded ethylene adsorbed on Pd(100) is thought to desorb reversibly, independent of the oxygen precoverage.<sup>8</sup>

The appearance of two molecular ethylene desorption peaks above the temperature of multilayer desorption (cf. Figure 3a,b) may be related to the local structures of the  $p(2\times 2)$  and  $p(1\times 2)$  oxygen overlayers. The 240 K peak appears with greater intensity in the ethylene thermal desorption spectra of the  $p(2\times 2)\text{O}$  overlayer than in those of the  $p(1\times 2)\text{O}$  overlayer, whereas the shoulder at 160 K appears with slightly greater intensity in the spectra of the  $p(1\times 2)\text{O}$  overlayer. These observations suggest that the 240 K peak may correspond to ethylene chemisorbed in areas with local  $p(2\times 2)\text{O}$  structure, whereas the 160 K peak may correspond to ethylene chemisorbed in areas with local  $p(1\times 2)\text{O}$  structure. If this interpretation is correct, the coverages of ethylene corresponding to these two thermal desorption peaks are indicative of the short-range perfection in these two ordered overlayers.

The desorption of  $\pi$ -bonded ethylene at 240 K occurs at a slightly higher temperature than that at which di- $\sigma$ -bonded ethylene desorbs molecularly.<sup>1</sup> The 240 K desorption temperature indicates that the strength of the ruthenium-ethylene  $\pi$ -bond is approximately 14 kcal/mol (perhaps slightly higher because of a small degree of rehybridization). The di- $\sigma$ -bonded ethylene has a slightly lower heat of adsorption (11 kcal/mol), but a higher binding energy of approximately 80 kcal/mol. This estimate takes into account the rehybridization that occurs upon adsorption using the known carbon-carbon and carbon-hydrogen bond energies of ethylene and ethane in the gas phase.

**B. Thermal Decomposition of Chemisorbed Ethylene.** As mentioned above, the  $\pi$ -bonded, molecularly chemisorbed ethylene that is observed on the Ru(001)- $p(2\times 2)\text{O}$  surface decomposes to a lesser extent than the di- $\sigma$ -bonded ethylene on the clean, the hydrogen-precovered ( $\theta_{\text{H}} = 0.25$ ), or the CO-precovered ( $\theta_{\text{CO}} = 0.25$ ) ruthenium surfaces. This difference results from the much stronger modification in the electronic structures of the surface by oxygen compared with hydrogen or CO. The primary effects of preadsorbed CO and hydrogen upon ethylene adsorption and reaction are to block the adsorption of ethylene and enhance molecular desorption relative to decomposition by blocking adsorption sites of the decomposition products.<sup>3</sup> On the other hand, oxygen adatoms modify the chemical nature of the surface qualitatively, thereby altering the nature of the molecular bonding of ethylene (from di- $\sigma$ - to  $\pi$ -bonding) and changing its decomposition products. For example,  $sp^2$ -hybridized vinylidene is observed as a product of the dehydrogenation of ethylene on Ru(001)- $p(2\times 2)\text{O}$ , whereas it is not observed on the reduced Ru(001) surface. It appears that  $sp^3$  hybridization and  $\eta^2$ -bonding are favored on Ru(001), upon which di- $\sigma$ -bonded ethylene and  $sp^3$ -hybridized acetylide are formed, and that  $sp^2$  hybridization and  $\eta^1$ -bonding are favored on the Ru(001)- $p(2\times 2)\text{O}$  surface, upon which  $\pi$ -bonded ethylene and  $sp^2$ -hybridized vinylidene are formed. Ethylidyne is observed on both Ru(001) ( $sp^3$  hybridization) and Ru(001)- $p(2\times 2)\text{O}$  ( $\eta^1$ -bonding). The presence of coadsorbed oxygen makes  $sp^3$  hybridization and  $\eta^2$ -bonding less favorable due, in part, to a weakening of the ruthenium-carbon bonds. This reduced bond strength is also manifest in less irreversible adsorption on the oxygen precovered surface: preadsorbed oxygen decreases the amount of ethylene that is adsorbed irreversibly in an approximately linear fashion.<sup>41</sup> Similar linear reductions in the extent of ethylene dehydrogenation by oxygen preadsorption have been observed on the Pd(100), Fe(111), and Pt(111) surfaces.<sup>8-10</sup>

Electron energy loss spectra of ethylene adsorbed on the Ru(001)- $p(2\times 2)\text{O}$  surface show that  $\pi$ -bonded ethylene reacts near 230 K to form ethylidyne, all of which dehydrogenates to an

(30) Anton, A. B.; Avery, N. R.; Toby, B. H.; Weinberg, W. H. *J. Am. Chem. Soc.* **1986**, *108*, 684.

(31) Anton, A. B.; Parmeter, J. E.; Weinberg, W. H. *J. Am. Chem. Soc.* **1986**, *108*, 1823.

(32) Parmeter, J. E.; Schwalke, U.; Weinberg, W. H. *J. Am. Chem. Soc.* **1987**, *109*, 1876.

(33) Parmeter, J. E.; Weinberg, W. H., to be published.

(34) Mulliken, R. S. *J. Chem. Phys.* **1979**, *71*, 556.

(35) Dance, D. F.; Walker, I. C. *Chem. Phys. Lett.* **1973**, *18*, 601.

(36) Demuth, J. E.; Eastman, D. E. *Phys. Rev. B* **1976**, *13*, 1523.

(37) Wandelt, K.; Hulse, J.; Küppers, J. *Surf. Sci.* **1981**, *104*, 212.

(38) Chan, C.-M.; Weinberg, W. H. *J. Chem. Phys.* **1979**, *71*, 2788.

(39) Feibelman, P. J. *Surf. Sci.* **1981**, *103*, L149.

(40) Parmeter, J. E., unpublished results.

(41) The inhibition of ethylene dissociation by oxygen atoms also results in part from oxygen blocking adsorption sites of the decomposition products.



sp<sup>2</sup>-hybridized vinylidene between 250 and 350 K with simultaneous desorption of hydrogen. It is rather likely that the  $\pi$ -bonded ethylene first dehydrogenates to vinylidene and that this vinylidene rehydrogenates to ethylidyne owing to the presence of surface hydrogen at temperatures below 250 K. This postulate is supported by EEL experiments, which showed that vinylidene coadsorbed with hydrogen could be rehydrogenated to ethylidyne.

In contrast to the partially irreversible adsorption of ethylene on the Ru(001)-p(2 $\times$ 2)O surface,  $\pi$ -bonded ethylene on Pd(100), precovered with 0.18 monolayer of oxygen forming a disordered overlayer, adsorbs reversibly,<sup>42</sup> and a variation in oxygen precoverage merely changes the ratio of di- $\sigma$ -bonded to  $\pi$ -bonded ethylene that is formed.<sup>8</sup> The di- $\sigma$ -bonded ethylene on Pd(100) dehydrogenates at 250 K to sp<sup>3</sup>-hybridized CHCH<sub>2</sub> which decomposes at higher temperatures to methylidyne. As shown by EELS, the  $\pi$ -bonded ethylene that is chemisorbed on Pt(111) with a fractional precoverage of 0.23 oxygen adatom forms a new, previously unidentified species upon annealing to 325 K.<sup>10</sup> Although spectra of the corresponding deuterated species are not available to confirm our assignment, we suggest that the  $\pi$ -bonded ethylene coadsorbed with a fractional coverage of 0.23 oxygen adatom on Pt(111) converts to an sp<sup>2</sup>-hybridized vinylidene. Indeed, the EEL spectrum of this vinylidene is very similar to that of vinylidene on Ru(001)-p(2 $\times$ 2)O. It exhibits an intense and broad loss feature at 1420 cm<sup>-1</sup> probably due to the (uncoupled)  $\delta$ (CH<sub>2</sub>) and  $\nu$ (CC) modes. The  $\nu_s$ (CH<sub>2</sub>) and  $\nu_a$ (CH<sub>2</sub>) modes appear at 2980 and 3080 cm<sup>-1</sup>, respectively. Other modes that appear at 940, 820, and 730 cm<sup>-1</sup> may be assigned to the CH<sub>2</sub> rocking, wagging, and twisting modes of vinylidene. On the Pt(111) surface, ethylene is di- $\sigma$ -bonded and converts to ethylidyne near 300 K, and it is possible that vinylidene on the oxygen-precovered surface may also be hydrogenated to ethylidyne. Hence, the interaction of ethylene with ruthenium precovered with a p(2 $\times$ 2)O overlayer is similar to that observed with platinum upon which a comparable fractional coverage of oxygen is present: on both surfaces,  $\pi$ -bonded ethylene converts to vinylidene. Both of these surfaces are more reactive than oxygen-precovered Pd(100).

As discussed in section III.B, the identification of adsorbed vinylidene on Ru(001)-p(2 $\times$ 2)O is confirmed by both EEL spectra and by hydrogen thermal desorption spectra, which show that the stoichiometry of the intermediate is C<sub>2</sub>H<sub>2</sub>. Note that the EEL spectra of Figure 4c,d cannot be attributed to chemisorbed acetylene owing to the absence in Figure 4c of the intense carbon-hydrogen bending mode at 765 cm<sup>-1</sup>, which is characteristic of acetylene chemisorbed on the Ru(001) and Ru(001)-p(2 $\times$ 2)O surfaces, and the observation of CH<sub>2</sub> and CD<sub>2</sub> scissoring modes at 1435 and 1010 cm<sup>-1</sup> in Figure 4c,d. The presence of methylidyne at this temperature can be ruled out because of the absence of an intense CH bending mode in the EEL spectrum of Figure 4c, which would be expected at 810 cm<sup>-1</sup>. The existence of CH<sub>3</sub> and CD<sub>3</sub> groups may also be excluded by examination of the EEL spectra. The vibrational frequencies of the adsorbed vinylidene agree with those of the vinylidene in the Os<sub>3</sub>(CO)<sub>9</sub>(CCH<sub>2</sub>)H<sub>2</sub> complex,<sup>22</sup> the bonding configuration and structure of which are shown in Figure 5a,b.<sup>25</sup> We would expect that the vinylidene is adsorbed similarly on the ruthenium surface with the CCH<sub>2</sub> bridge-bonded, the carbon-carbon bond axis tilted with respect to the surface normal, elongation of the carbon-carbon bond compared with that of gaseous ethylene, and some donation of electron density from the  $\pi$  orbital of the CCH<sub>2</sub> to the d band of the ruthenium surface (cf. Figure 5c). The observed  $\nu$ (CC) mode of adsorbed CCH<sub>2</sub> at 1435 cm<sup>-1</sup> is lowered from those of C<sub>2</sub>H<sub>4</sub>(g) at 1623 cm<sup>-1</sup> and the CCH<sub>2</sub> ligand in Cp<sub>2</sub>Ru<sub>2</sub>(CO)<sub>2</sub>( $\mu$ -CO)( $\mu$ -CCH<sub>2</sub>) at 1586 cm<sup>-1</sup>,<sup>43</sup> owing to the  $\pi$ -electron donation from the carbon-carbon bond to the metal surface that occurs in the chemisorbed vinylidene. The overlap of the  $\nu$ (CC) and  $\delta$ (CH<sub>2</sub>) modes of adsorbed vinylidene at 1435 cm<sup>-1</sup> indicates that

these modes are not coupled significantly in this species, unlike those of  $\pi$ -bonded ethylene. It cannot be entirely ruled out that the  $\nu$ (CC) mode appears at a slightly lower frequency than 1435 cm<sup>-1</sup>, and that the  $\delta$ (CH<sub>2</sub>) mode "steals" intensity from the  $\nu$ (CC) mode via mode coupling. However, the absence of any evidence for a shoulder on the low-frequency side of the peak at 1435 cm<sup>-1</sup> in Figure 4c makes this unlikely.

Gates and Kesmodel<sup>23</sup> have suggested the presence on the Pd(111) surface of a CCH<sub>2</sub> adspecies as an intermediate to the formation of ethylidyne from hydrogen and acetylene. This postulated CCH<sub>2</sub> adspecies was coadsorbed with acetylene, hydrogen, and ethylidyne. Thus, only two of the vibrational modes were identified,  $\nu$ (CC) and/or  $\delta$ (CH<sub>2</sub>) at 1437 cm<sup>-1</sup> and  $\nu$ (CH<sub>2</sub>) at 2986 cm<sup>-1</sup> [ $\nu$ (CC) at 1372 cm<sup>-1</sup> and  $\nu$ (CD<sub>2</sub>) at 2206 cm<sup>-1</sup> for CCD<sub>2</sub>]. A CCH<sub>2</sub> adspecies, an intermediate in the hydrogenation of acetylene to ethylidyne on Pt(111), was tentatively identified by Ibach and Lehwald<sup>24</sup> with mode assignments listed in Table II. The assignment of the carbon-carbon stretching mode to a loss feature at 1100 cm<sup>-1</sup> suggests sp<sup>3</sup> hybridization of the carbon atoms of the CCH<sub>2</sub> on Pt(111), indicating that this species is quite different from the sp<sup>2</sup>-hybridized CCH<sub>2</sub> species observed on Ru(001)-p(2 $\times$ 2)O and the oxygen-precovered Pt(111) surfaces. The change in hybridization of the CCH<sub>2</sub> species on platinum due to the presence of oxygen supports our earlier assertion that sp<sup>3</sup> hybridization is preferred on clean metal surfaces, whereas sp<sup>2</sup> hybridization is preferred in the presence of oxygen. Moreover, the observed conversion of CCH<sub>2</sub> to ethylidyne on palladium and platinum agrees with our observation that the conversion of ethylidyne to vinylidene is reversible on Ru(001), provided sufficient hydrogen is present.

The thermal evolution of  $\pi$ -bonded ethylene on Ru(001)-p(2 $\times$ 2)O can be summarized as follows. The ethylene reacts to form ethylidyne, possibly via a vinylidene intermediate, below 250 K. In contrast to the total dehydrogenation of ethylidyne to carbon with the simultaneous evolution of hydrogen with no stable intermediate on the Ru(001) surface, the ethylidyne on the Ru(001)-p(2 $\times$ 2)O surface dehydrogenates to vinylidene upon annealing to 350 K. The vinylidene decomposes to methylidyne and carbon adatoms evolving hydrogen between 350 and 450 K, possibly through an unstable acetylide intermediate. Acetylide, which was observed following the adsorption of ethylene on the Ru(001) surface, also decomposes via carbon-carbon bond cleavage to methylidyne at approximately the same temperature at which vinylidene decomposes on the Ru(001)-p(2 $\times$ 2)O surface. The methylidyne that is formed on Ru(001)-p(2 $\times$ 2)O decomposes between 500 and 700 K. Finally, the carbon reacts with oxygen adatoms to form CO, which desorbs in a reaction-limited step between 500 and 750 K.

The hydrogen thermal desorption spectra from ethylene chemisorbed on the Ru(001)-p(2 $\times$ 2)O surface are completely consistent with this decomposition mechanism. Hydrogen that is evolved from the ethylene and ethylidyne decomposition reactions desorbs in two peaks at 210 and 250 K. These two peaks account for half of the hydrogen desorption from the surface, consistent with the stoichiometry of the vinylidene intermediate observed on the surface at 350 K. The hydrogen thermal desorption peak at 400 K corresponds to one-quarter of the total amount of hydrogen that is desorbed and is therefore consistent with the dehydrogenation of vinylidene to methylidyne and carbon adatoms. The final quarter of the hydrogen desorbs above 500 K as the methylidyne decomposes.

Only C<sub>2</sub>H<sub>4</sub>, H<sub>2</sub> and CO were observed to desorb following the chemisorption of ethylene on the Ru(001)-p(2 $\times$ 2)O surface. This result is similar to the coadsorption of ethylene and oxygen on Fe(111), but unlike the coadsorption of ethylene and oxygen on Pd(100) and Pt(111), which exhibited CO<sub>2</sub> and H<sub>2</sub>O desorption as well.<sup>8-10</sup> The absence of CO<sub>2</sub> and H<sub>2</sub>O in the thermal desorption spectra from the ruthenium surface is not surprising since neither the formation of CO<sub>2</sub> from coadsorbed CO and oxygen<sup>44</sup> nor the formation of water from coadsorbed oxygen and hydrogen has

(42) As shown by EELS, the irreversibly adsorbed ethylene on the Pd(100) surface preexposed to oxygen is di- $\sigma$ -bonded.<sup>8</sup>

(43) Evans, J.; McNulty, G. S. *J. Chem. Soc., Dalton Trans.* **1983**, 639.

(44) Thomas, G. E.; Weinberg, W. H. *J. Chem. Phys.* **1979**, *70*, 954.



been observed under UHV conditions on the Ru(001) surface in transient thermal desorption experiments.<sup>45</sup> The lower reactivity of ruthenium and iron for the oxidation of carbon monoxide and hydrogen is a consequence of the stronger metal-oxygen bonds that are formed<sup>6,46</sup> compared with those of platinum<sup>47</sup> and palladium.<sup>48</sup>

Finally, the chemistry of ethylene on the Ru(001)-p(2×2)O surface may be compared to the organometallic chemistry of homogeneous compounds. For example, it has been shown that ethylene reacts with Os<sub>3</sub>(CO)<sub>12</sub> to form the vinyl complex, HOs<sub>3</sub>(CH=CH<sub>2</sub>)(CO)<sub>10</sub>, which forms the vinylidene complex, H<sub>2</sub>Os<sub>3</sub>(CO)<sub>9</sub>(C=CH<sub>2</sub>)<sup>22</sup> upon heating. The latter can be hydrogenated to an ethylidyne complex, H<sub>3</sub>Os<sub>3</sub>(CO)<sub>9</sub>(CCH<sub>3</sub>),<sup>22,25,49</sup> just as chemisorbed vinylidene can be rehydrogenated to ethylidyne on the Ru(001)-p(2×2)O surface. These results also suggest that the conversion of π-bonded ethylene to vinylidene on Ru(001)-p(2×2)O occurs via a vinyl intermediate.

## V. Conclusions

The presence of ordered p(2×2) and p(1×2) oxygen overlayers on the Ru(001) surface gives rise to π-bonding of molecularly chemisorbed ethylene, such that the carbon atoms of the ethylene remain nearly sp<sup>2</sup>-hybridized. This species is qualitatively different from the sp<sup>3</sup>-hybridized, di-σ-bonded ethylene that is observed on the clean surface. Intuitively, this difference reflects the greater Lewis acidity of the Ru(001)-p(2×2)O and Ru(001)-p(1×2)O surfaces. More precisely, it is a consequence of a significant perturbation in the electronic structure of the ruthenium surface by the ordered oxygen overlayers, which increases the energy

(45) Hills, M. M., unpublished results.

(46) Seip, U.; Tsai, M.-C.; Christmann, K.; Küppers, J.; Ertl, G. *Surf. Sci.* **1984**, *139*, 29.

(47) Avery, N. R. *Chem. Phys. Lett.* **1983**, *96*, 371.

(48) Nyberg, C.; Tengstäl, C. G. *Surf. Sci.* **1983**, *126*, 163.

(49) Deeming, A. J.; Underhill, M. J. *Chem. Soc., Chem. Commun.* **1973**, 277.

separation between the Fermi level and the π\* orbital of ethylene, making back-donation unfavorable.

As observed on the oxygen-precovered Pt(111), Pd(100), and Fe(111) surfaces, a larger fraction [one-third on Ru(001)-p(2×2)O] of π-bonded ethylene desorbs molecularly than does di-σ-bonded ethylene on the reduced surfaces. The remaining two-thirds of the saturation coverage of ethylene adsorbed on the Ru(001)-p(2×2)O surface dehydrogenates to ethylidyne probably via a vinylidene intermediate upon heating to 250 K. In contrast to the observed total decomposition of ethylidyne to carbon and hydrogen on the Ru(001) surface with no stable intermediates, the presence of oxygen induces the formation of an sp<sup>2</sup>-hybridized vinylidene species from ethylidyne at 350 K. By analogy to the H<sub>2</sub>Os<sub>3</sub>(CO)<sub>9</sub>(CCH<sub>2</sub>) cluster,<sup>22,25,49</sup> this chemisorbed vinylidene is almost certainly bridge-bonded to two adjacent ruthenium atoms and tilted toward a third ruthenium atom with donation of electron density from the π orbital to the d band of the ruthenium surface, as shown in Figure 5c. The chemisorbed vinylidene decomposes near 400 K to carbon adatoms and methylidyne, the latter of which dehydrogenates between 500 and 700 K. The vinylidene could be rehydrogenated to ethylidyne in the presence of hydrogen, analogous to the formation of ethylidyne from CCH<sub>2</sub> on reduced Pt(111) and Pd(111).<sup>23,24</sup> No oxygen-containing intermediates in ethylene decomposition were observed under any conditions of temperature and coverage. Oxygen adatoms reacted only with carbon adatoms, forming CO above 500 K.

Finally, the presence of oxygen favors η<sup>1</sup>-bonding and sp<sup>2</sup> hybridization as shown by both the existence of π-bonded ethylene on the oxygen-precovered Pt(111), Pd(100), Fe(111), and Ru(001) surfaces,<sup>8-11</sup> as well as the formation of sp<sup>2</sup>-hybridized vinylidene on these chemically modified Ru(001) and Pt(111) surfaces.<sup>10</sup> On the other hand, η<sup>2</sup>-bonded, sp<sup>3</sup>-hybridized ethylene was observed in the absence of oxygen on all four surfaces.

**Acknowledgment.** This work was supported by the National Science Foundation under Grant No. CHE-8516615.

## Infrared Matrix Isolation Study of Hydrogen Bonds Involving C-H Bonds: Alkynes with Oxygen Bases

Andrea M. DeLaat and Bruce S. Ault\*

Contribution from the Department of Chemistry, University of Cincinnati, Cincinnati, Ohio 45221. Received January 2, 1987

**Abstract:** The hydrogen-bonded complexes of acetylene and a set of related alkynes with a series of oxygen-containing bases have been isolated in inert matrices at 14 K and characterized by infrared spectroscopy. Coordination of the acetylenic hydrogen to the oxygen atom of the base was evidenced by shifts of the C-H stretching mode,  $\nu_s$ , to lower energies. These shifts, in the range of 50–100 cm<sup>-1</sup>, were smaller than those observed previously for hydrogen-bonded complexes. Nonetheless, the shifts were distinct and variable with the different alkynes and bases employed, indicating the accessibility of a range of complexes. For example, the codeposition of propyne with (CH<sub>3</sub>)<sub>2</sub>O, (CH<sub>3</sub>)<sub>2</sub>CO, (CH<sub>3</sub>)<sub>2</sub>O, and (CH)<sub>4</sub>O gave rise to a perturbed C-H stretching mode shifted 71, 64, 55, and 16 cm<sup>-1</sup> from the parent C-H stretching mode, respectively. The shifts for the substituted alkynes varied in the order phenylacetylene > *tert*-butylacetylene > 1-butyne > propyne, consistent with gas-phase acidity data.

Hydrogen bonding has been a subject of great interest to chemists over the years, as its importance to many areas of chemistry has long been recognized.<sup>1</sup> As a result of this interest, much study has been directed toward a more complete understanding of this very important molecular interaction. Despite much experimental effort and theoretical discussion, the details of hydrogen bonding are by no means completely understood.

The most frequent participants in hydrogen bonding are the highly electronegative elements N, O, and F, although elements of lesser electronegativity have been studied as well. The ability of group IVA elements to participate in hydrogen bonding, particularly carbon and silicon, has also generated substantial experimental and theoretical interest.<sup>2-5</sup> It is generally accepted

\* Author to whom correspondence should be addressed.

(1) Pimentel, G. C.; McClellan, A. L. *The Hydrogen Bond*; W. H. Freeman Co.: San Francisco, 1960.